RECENT IMPROVEMENT OF TRACKING CODE BBSIMC

H. J. Kim and T. Sen, Fermi National Accelerator Laboratory, Batavia, Illinois 60510, USA

Abstract

The beam-beam simulation code (BBSIMC) is a incoherent multiparticle tracking code for modeling the nonlinear effects arising from beam-beam interactions and the compensation of them using an electromagnetic lens. It implements short range transverse and longitudinal wakefield, dipole noise to mimic emittance growth from gas scattering, beam transfer function, and wire compensation models. In this paper, we report on recent improvements of the BBSIMC including a beam-beam compensation model using a low energy electron beam and a current carrying wire.

INTRODUCITON

A beam-beam simulation code BBSIMC has been developed at FNAL over the past few years to study the effects of the machine nonlinearities and the beam-beam interactions. The code is under continuous development with the emphasis being on including the important details of an accelerator and the ability to reproduce observations in diagnostic devices. At present, the code can be used to calculate tune footprints, dynamic apertures, beam transfer functions, frequency diffusion maps, action diffusion coefficients, emittance growth and beam lifetime. Calculation of the last two quantities over the long time scales of interest is time consuming even with modern computer technology. In order to run efficiently on a multiprocessor system, the resulting model was implemented by using parallel libraries which are MPI (interprocessor Message Passing Interface standard) [**?**], state-of-the-art parallel solver libraries (Portable, Extensible Toolkit for Scientific Calculation, PETSc) [**?**], and HDF5 (Hierarchical Data Format) [**?**]. The following section describes the physical model used in the simulaiton code. Some applications are presented for the Large Hadron Collider (LHC) wire compensator and the Relativistic Heavy Ion Collider (RHIC) electron lens.

PHYISCAL MODEL

In the collider simulation, the two beams moving in opposite direction are represented by macroparticles of which the charge to mass ratio is that of each beam. Fewer number of macroparticles are chosen than bunch intensity of the beam because it becomes prohivitive for few revolutions around accelerator even with modern supercomputers. They are genernated and loaded with an initial distribution for a specific simulation purpose according to the beam parameters at the interaction point, for example, six-dimensional Gaussian distribution for long-term beam evolution. The transverse and longitudinal motion of particles is calculated by transfer maps which consist of linear and nonlinear maps. In the simulations, the following nonlinearity is included: head-on and long-range beam-beam interactions, external electromagnetic force by current carrying wire, mulitipole errors due to quadrupole triplets, and sextupole strength of chromaticity correction. In the following, linear and nonlinear tracking models are described in detail.

Transportation through arc

The six-dimensional accelerator coordinates $\mathbf{x} = \left(x, x^{'}, y, y^{'}, z, \delta\right)^T$ are applied, where x and y are horizontal and vertical coordinates, $x^{'}$ and $y^{'}$ the trajectory slopes of each coordinates, $z = -c\Delta t$ the longitudinal distance from syncrhotron particle, and $\delta = \Delta p_z/p_0$ the momentuem deviation from the synchrotron. The linear rotation between two elements denoted by i and j can be written as

$$\mathbf{x}_j = \begin{pmatrix} \mathcal{M} & \hat{\mathcal{D}} \\ 0 & \mathcal{L} \end{pmatrix} \mathbf{x}_i. \tag{1}$$

Here, $\mathcal{M}$ is coupled transverse map of *off-momentum* motion defined by $\mathcal{M} = \mathcal{R}_j \tilde{\mathcal{M}}_{i\to j} \mathcal{R}_i^{-1}$, where $\tilde{\mathcal{M}}_{i\to j}$ is the uncoupled linear map described by twiss functions at i and j elements, and the transverse coupling matrix $\mathcal{R}$ is defined as

$$\mathcal{R} = \frac{1}{\sqrt{1+|C|}} \begin{pmatrix} I & C^\dagger \\ -C & I \end{pmatrix}, \tag{2}$$

where $C^\dagger$ is the 2×2 matrix and the symplectic conjugate of the coupling matrix C. The dispersion matrix is described by $\hat{\mathcal{D}} = (0, \mathbf{D})$, and the dispersion vector $\mathbf{D} = \left(D_x, D_{x'}, D_y, D_{y'}\right)$ is characterized by the transverse dispersion functions and the map $\mathcal{M}$:

$$\mathbf{D} = \mathbf{D}_j - \mathcal{M}\mathbf{D}_i. \tag{3}$$

$\mathcal{L}$ is a longitudinal map and a nonlinearity of synchrotron oscillations is applied by adding the longitudinal momentum change at rf cavity.

Beam-beam interactions

For head-on and long-range beam-beam interactions, we assume that one beam is strong and is not affected by the other beam while the other beam is weak and experiences a beam-beam force due to the strong beam during the collision, so called weak-strong beam-beam model. Besides, the charge distribution of the strong beam is assumed to be

Gaussian:

$$\rho(x,y,z) = \frac{nq}{(2\pi)^{3/2}\sigma_x\sigma_y\sigma_z}\exp\left(-\frac{x^2}{2\sigma_x^2}-\frac{y^2}{2\sigma_y^2}-\frac{z^2}{2\sigma_z^2}\right), \quad (4)$$

where n is the number of particles and q is the electric charge of the beam. Note that the coordinates (x,y,z), denote the rest frame of the strong beam. The beam-beam force between two beams with transverse Gaussian distribution $\rho(x,y) = \int dz\rho(x,y,z)$ is well-known, and the expression for the slope change is given by, for elliptical beam with $\sigma_x > \sigma_y$:

$$\Delta x' = \frac{2\tilde{n}r_0}{\gamma}\frac{\sqrt{\pi}}{\sqrt{2\left(\sigma_x^2-\sigma_y^2\right)}}\Im F(x,y), \quad (5a)$$

$$\Delta y' = \frac{2\tilde{n}r_0}{\gamma}\frac{\sqrt{\pi}}{\sqrt{2\left(\sigma_x^2-\sigma_y^2\right)}}\Re F(x,y), \quad (5b)$$

where $F(x,y)$ is a complex function defined in [**?**]. New constants are defined as $r_0 \equiv qq_*/4\pi\epsilon_0 m_0 c^2$ and $\tilde{n} \equiv n\left(\left|\vec{\beta}\right|^{-1}+\left|\vec{\beta}_*\right|\right)/\left(\left|\vec{\beta}\right|+\left|\vec{\beta}_*\right|\right)$. Here, a subsript asterisk designates a variable of weak beam.

Electromagetic lens

It is well known that for a large separation distance ($\gg\sigma$) at parasitic crossings, the strength of long-range interactions is inversely proportional to the distance. Its effect on a test beam can be compensated by current carrying wires which create just the $\frac{1}{r}$ field. The advantage of such an approach consists of the simplicity of the method and the possibility to deal with all multipole orders at once. For a finite length l_w embedded in the middle of a drift length L, the transfer map of a wire can be obtained by

$$\mathcal{M}_w^{(L)} = D_{L/2}\circ\mathcal{M}_k^{(L)}\circ D_{L/2}, \quad (6)$$

where $D_{L/2}$ is the drift map with a length $\frac{L}{2}$, and $\mathcal{M}_k^{(L)}$ is the wire kick integrated over a drift length. The change in slopes of a test beam is

$$\begin{pmatrix}\Delta x'\\ \Delta y'\end{pmatrix} = \frac{\mu_0}{4\pi}\frac{I_w l_w}{(B\rho)}\frac{u-v}{x^2+y^2}\begin{pmatrix}x\\ y\end{pmatrix}, \quad (7)$$

where I_w is the current of wire , u and v are $\sqrt{\left(\frac{L}{2}+l_w\right)^2+x^2+y^2}$ and $\sqrt{\left(\frac{L}{2}-l_w\right)^2+x^2+y^2}$ respectively. Besides, we take into account the wire placement including pitch and yaw angles. The transfer map of wire can be written by

$$\mathcal{M}_w = D_{-L/2}\circ S_{\Delta x,\Delta y}\circ T^{-1}_{\theta_x,\theta_y}\circ D_{L_2}\circ\mathcal{M}_k \circ D_{L_1}\circ T_{\theta_x,\theta_y}\circ D_{-L/2}, \quad (8)$$

where T_{θ_x,θ_y} represents the tilt of the coordinate system by horizontal and vertical angles θ_x,θ_y to orient the coordinate system parallel to the wire, and $S_{\Delta x,\Delta y}$ represents a shift of the coordinate axes to make the coordinate systems after and before the wire agree. When the wire is parallel to the beam, Eq. (**??**) becomes $\mathcal{M}_w = \mathcal{M}_k$. For cancelling the long-range beam-beam interactions of the round beam with the wire, one can get the desired wire current and length; the integrated strength of the wire compensator should be commensurate with the integrated current of the beam bunch, i.e., $I_w l_w = cq_* n_*$.

Electron lens

An electron lens is expected to improve beam lifetime and luminosity of the colliding beams by reducing the betatron tune shift and spread from the head-on collisions. A space charge force of low-energy electron beam is acting as a focusing or defocusing lens depending on the high energy bunches. In `BBSIMC`, two electron beam distribution functions are implemented: (a) Gaussian distribution and (b) Smooth-edge-flat-top (SEFT) distribution. The transverse kick on the high energy beam from the electron beam is given by

$$\Delta\vec{r'} = \frac{2\tilde{n}r_0}{\gamma}\frac{\vec{r}_\perp}{r_\perp^2}\zeta(r_\perp:\bar{\sigma}),$$

where $\tilde{n}$ is the number of electrons of the electron beam adjusted by the electron speed, r_0 is the classic particle radius, $\bar{\sigma}$ is the electron beam size, and γ is the Lorentz factor. The function ζ is given by

- for Gaussian distribution

$$\zeta(r_\perp:\bar{\sigma}) = \left[1-\exp\left(-\frac{r_\perp^2}{2\bar{\sigma}^2}\right)\right],$$

- for SEFT distribution

$$\zeta = \frac{\sqrt{2}\tilde{\rho}_0}{8}\left[\frac{1}{2}\log\left(\frac{\theta_+^2+1}{\theta_-^2+1}\right)+\tan^{-1}\theta_+ +\tan^{-1}\theta_-\right],$$

where $\tilde{\rho}$ is a constant, and $\theta_\pm = \sqrt{2}\left(\frac{r}{\bar{\sigma}}\right)^2 \pm 1$.

Finite bunch length

The bunch length effect needs to be considered in case of (1) the longitudinal bunch length σ_z is comparable to the transverse lengths σ_x and σ_y, (2) the orbit function β_x and β_y are not constant through beam-beam interactions, and (3) the transverse beta functions are small and comparable to σ_z. We make slices of both beams moving in opposite directions. Each slice is integrated over its longitudinal boundary, and has only transverse charge distribution at the center of its longitudinal boundary. We take into account the collision between a pair of slices: each slice in a beam interacts with particles in the other beam in turn at the collision points. In additon, electric field energy varies along the bunch due to the inhomogenity of beam parameters in the longitudianal direction, and couples transverse and longitudinal motions. The coupling can be modelled by including beam-beam interactions due to the longitudinal component of the electric field as well as the transverse components [**?**].

Particle Loading

At the start of the simulation, the particles in the weak beam are distributed over the phase space. The number of simulation particles is limited by the computational power. In order to make the best use of a relatively small number of simulation particles compared to the bunch intensity, the initial distribution should be optimized. Indeed the initial distribution is very important because a proper choice can reduce the statistical noise in the physical quantities. The simulation particles are generated in two steps: (i) The particle coordinates (x, y, z) of particles can be directly generated from the spatial Gaussian distribution, $\bar{\rho}(x, y, z) = \bar{\rho}_x(x)\,\bar{\rho}_y(y)\,\bar{\rho}_z(z)$, where $\bar{\rho}_\zeta(\zeta) = \bar{\rho}_{\zeta 0}\exp\left(-\frac{\zeta^2}{2\sigma_\zeta^2}\right)$. Since the particle coordinates are not correlated, one can generate them by inverse mapping of each cumulative distribution function of horizontal, vertical, and longitudinal Gaussian distributions, using bit-reversed sequence to minimize nonphysical correlations [**?**]. (ii) An equilibrium distribution in transverse phase space e.g. in the (x, x') plane is $\hat{\rho}\left(x, x^{'}\right) = \hat{\rho}_0 \exp\left(-\frac{x^2+\left(\beta_x x^{'}+\alpha_x x\right)^2}{2\sigma}\right)$. Since the spatial coordinate x is determined at the first step, the slope $x^{'}$ can be obtained from the random variate r of a univariable Gaussian, i.e., $x^{'} = (r - \alpha_x x)/\beta_x$.

APPLICATIONS

LHC

Long-range beam-beam interactions are known to cause emittance growth or beam loss in the Tevatron and are expected to deteriorate beam quality in the LHC. Increasing the crossing angle to reduce their effects has several undesirable effects, the most important of which is a lower luminosity due to the smaller geometric overlap. For the LHC, a wire compensation scheme has been proposed to compensate the long-range interactions by applying external electromagnetic forces. At large beam-beam separation, the electromagnetic force which a beam exerts on individual particles of the other beam is proportional to $\frac{1}{r}$, which can be generated and canceled out by the magnetic field of a current-carrying wire. However, several issues need to be resolved for efficient compensation. With the present bunch spacing, there are about 30 long-range interactions on both sides of an interaction point (IP). The beam-beam separation distance varies from 6.3 σ to 12.6 σ. The resulting beam-beam force is not identical to that generated by a single or multiple wire(s).

The wire-beam separation distance is one of major parameters which determine the performance of a wire compensator. Figure **??** shows the angle-averaged dynamic aperture for off-momentum particles with 3 $\sigma_{\Delta p/p}$ for different wire-beam separations. The reference separation (9 σ) is choen as the average of beam-beam separations. The dynamic aperture calculated at different phase angles is the largest radial amplitude of particles that survive up to a certain time interval; in this simulation, 10^6 turns. When the beam-beam compensation is not present, the dynamic aperture is around 8 σ. However, for a wide separation range, the dynamic aperture is smaller than 8 σ by about 2-4 σ. The dynamic aperture decrease linearly as the separation decreases. Figure **??** shows the results of particle loss in 1×10^6 turns for different wire-beam separations. The particle loss saturates at large separation while there is a sharp increase of particle loss at small separation. We directly see the minimum particle loss between 0.9 and 1.0 of the reference separation. It reveals that the average of beam-beam separations is close to an optimal separation between the wire and the high energy bunch.

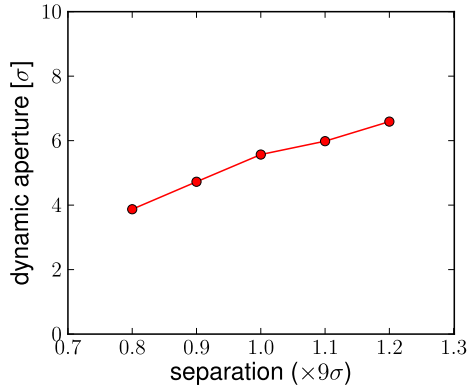

Figure 1: Plot of angle-averaged dynamic apertures according to wire separation distance with wire strength 82.8 Am.

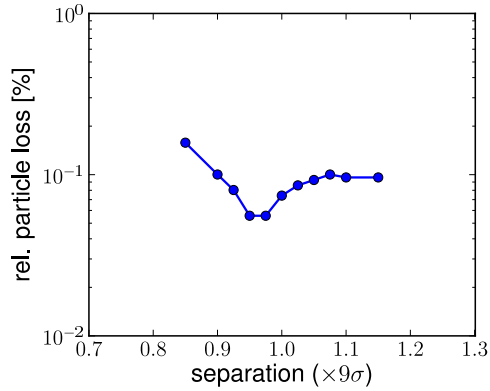

Figure 2: Plot of particle loss according to wire-beam separation distance with wire strength 82.8 Am.

RHIC

Increasing the luminosity requires higher beam intensity and often focusing the beam to smaller sizes at the interaction points. The effects of head-on interactions become even more significant. The head-on interaction introduces a tune spread due to a difference of tune shifts between small and large amplitude particles. In the proton-proton run of RHIC, the maximum beam-beam parameter reached so far is about $\xi = 0.008$. The combination of beam-beam and

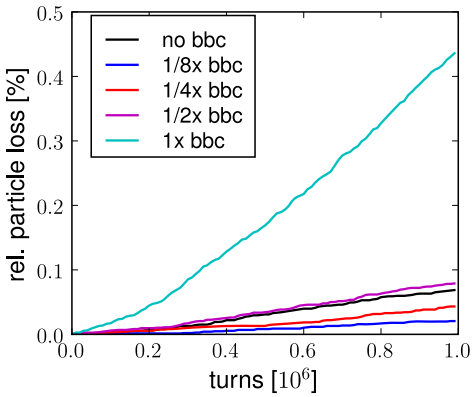

Figure 3: Plot of particle loss according to electron beam intensity for a 1σ Gaussian electron beam profile .

Profile	Intensity (4×10^{11})	DA (σ)	Particle loss† (%)
1σ Gaussian	1	4.48	635
	1/2	5.10	115
	1/4	5.44	63
	1/8	5.63	30
2σ Gaussian	4	3.53	93
	2	5.05	10
	1	5.40	8
	1/2	5.63	6
SEFT	8	3.60	330
	4	4.77	21
	2	5.46	22
	1	5.47	6
	1/2	5.57	6

†relative to that without beam-beam compensation

Table 1: Comparison of dynamic apertures and particle loss for different electron beam profiles and intensities.

machine nonlinearities excite betatron resonances which diffuse particles into the tail of beam distribution and even beyond the stability boundary. It is therefore important to mitigate the head-on beam-beam effect.

In order to seek the electron lens parameters at which the beam life time is improved, we choose three different electron beam distribution functions: (a) 1σ Gaussian distribution with the same rms beam size as that of the proton beam σ, (b) 2σ Gaussian distribution with rms size twice that of the proton beam, and (c) Smooth-edge-flat-top (SEFT) distribution with an edge around at 4 σ. When the electron beam profile matches the proton beam, the full compression of the tune spread requires the electron beam intensity $N_e = 4 \times 10^{11}$ which is defined as the electron beam intensity required for full compensation or 1x bbc. Figure **??** shows the results of particle loss for different intensities with the 1σ Gaussian electron beam profile. At an intensity of 1x bbc, the particle loss is nearly six times the loss without beam-beam compensation. The beam lifetime of $\frac{1}{2}$x bbc however is comparable with that of no bbc. As the electron beam intensity is decreased, the particle loss decreases significantly below $\frac{1}{4}$x bbc, and is reduced to 30% of no bbc at $\frac{1}{8}$x bbc.

For the 2σ Gaussian and SEFT electron beam profiles, we calculated dynamic apertures and particle loss for different electron beam intensities. The results are summarized in Table **??**. The upper limits of the electron beam intensity for the two distributions are chosen so that peak of the electron profile is matched to that of 1x bbc at 1σ Gaussian. For the $\frac{1}{2}$x bbc and 1x bbc of 2σ Gaussian profile, there is a small increase in the dynamic aperture of off-momentum particles. There is however a significant reduction in beam loss, for example, below 10% of the particle loss without beam-beam compensation when the electron beam intensity is $\frac{1}{2}$x bbc. The dynamic aperture obtained with the SEFT profile remains almost the same up to 2x bbc. Nevertheless a significant improvement of beam lifetime is also observed below 2x bbc. There is a threshold electron beam intensity below which beam life time is increased: $\frac{1}{2}$x bbc for the 1σ Gaussian, 2x bbc for the 2σ Gaussian, and 4x bbc for the SEFT profile. Particle loss is relatively insensitive to electron lens current variations below threshold current with the 2σ Gaussian and SEFT profiles. This looser tolerance on the allowed variations in electron intensity is likely to be beneficial during experiments.

SUMMARY

In order to study the effects of the machine nonlinearities and the beam-beam interactions, and the effectiveness of compensation schemes of beam-beam interactions, we have developed a six-dimensional weak-strong code BBSIMC. The simulations are carried out using both LHC and RHIC. The results of LHC simulation show that the particle loss is minimized at the wire separation which corresponds to the average of beam-beam separations. We observed, from the redults of RHIC, that there is a threshold electron beam intensity below which proton beam life time is increased. A wider electron beam profile than the proton beam at the electron lens location is found to increase beam life time.

REFERENCES

[1] M. Bassetti and G.A. Erskine, CERN-IRS-TH/80-06, CERN (1980).

[2] MPI-2: Extensions to the Message-Passing Interface, U. of Tennessee, Knoxbille, TN (2003).

[3] S. Balay, at al, Tech. Rep. ANL-95/11 - Revision 2.3.3, ANL (2008).

[4] *HDF5 User's Guid*, NCSA, UIUC, Urbana, IL (2005).

[5] H.J. Kim and T. Sen, in *Proceedings of PAC09*, WE6PFP032.

[6] K. Hirata, H. Moshammer, and F. Ruggiero, Particle Accel. **40**, 205 (1993).

[7] C.K Birdsall and A.B. Langdon, *Plasma Physics via Computer Simulation* (McGraw-Hill, 1985).